

# Exploring colourful holographic superconductors

---

**Kasper Peeters, Jonathan Powell and Marija Zamaklar**

*Department of Mathematical Sciences,  
Durham University,  
South Road,  
Durham DH1 3LE,  
United Kingdom.*

kasper.peeters@durham.ac.uk  
jonathan.powell@durham.ac.uk  
marija.zamaklar@durham.ac.uk

**ABSTRACT:** We explore a class of holographic superconductors built using non-abelian condensates on probe branes in conformal and non-conformal backgrounds. These are shown to exhibit behaviour of the specific heat which resembles that of heavy fermion compounds in the superconducting phase. Instead of showing BCS-like exponential behaviour, the specific heat is polynomial in the temperature. It exhibits a jump at the critical temperature, in agreement with real-world superconductors. We also analyse the behaviour of the energy gap and the AC and DC conductivities, and find that the systems can be either semi-conducting or metallic just above the critical temperature.

**KEYWORDS:** AdS/CFT, phase transitions, superconductivity.

---

## Contents

<b>1. Introduction and summary</b>	<b>1</b>
<b>2. Colourful superconductors</b>	<b>3</b>
2.1 Non-abelian condensates	3
2.2 Overview of the models	4
2.3 Comments on the zero temperature limit	7
<b>3. Thermodynamic properties</b>	<b>8</b>
3.1 Free energy and specific heat	8
3.2 Limitations of the Yang-Mills approximation	10
3.3 Comments on connections with real-world superconductors	11
<b>4. Electromagnetic properties</b>	<b>13</b>
4.1 AC conductivity	13
4.2 DC conductivity	16
4.3 Comments on connections with real-world superconductors	18
<b>A. Appendix: computing temperature dependence</b>	<b>20</b>

---

## 1. Introduction and summary

An intriguing new application of the correspondence between string theory and gauge theory is the study of strongly coupled systems which exhibit superconductivity. Apart from suggesting an alternative point of view on non-BCS superconductors, these might also help to develop a better understanding of quantum critical points and strongly coupled superconductors for which so far a satisfactory theory is lacking [1]. Moreover, these constructions provide an interesting new arena in which to explore and test the string/gauge theory correspondence. We refer the reader to [2, 3] for more background information and references.

In the original model of [1], a holographic superconductor was constructed by considering an Abelian Higgs model in the background of an anti-de-Sitter black hole. A stable condensate of the scalar field can occur because of nontrivial coupling of the scalar to the gauge potential, in combination with nontrivial asymptotics [4] or because of the nontrivial near-horizon geometry which destabilises the asymptotically stable mode [1]. This system exhibits an energy gap which scales linearly with the critical temperature, and a frequency-dependent conductivity which shows some similarity with real-world superconductors. A full analysis involving back-reaction of the Abelian-Higgs fields on the gravitational background has also been carried out [5].

A different way to obtain a non-trivial condensate in a holographic setup is to consider, instead, a non-abelian gauge field coupled to gravity. Again, because of the non-trivial asymptotics, it is possible to form condensates of the gauge field. For some time now, it has been known that such configurations exist even in systems at zero temperature (i.e. without black hole horizon), where they are related to vector meson condensates in the dual gauge theory [6]. An application to  $p$ -wave superconductors was developed in [4], based on earlier work in [7]. We will call these ‘colourful superconductors’ (not to be confused with colour superconductors in QCD).

Many properties of these colourful superconductors have so far not been analysed, and it is far from clear which real-world superconductors they resemble most. Moreover, the analysis so far has focussed on *conformal* cases, since there is an expectation that ideas of the gauge/gravity correspondence are perhaps most useful in the context of quantum critical phenomena, which are often characterised by relativistic conformal symmetry.

In the present paper we thus set out to investigate a variety of models which exhibit non-abelian condensates. We will focus mostly on D-brane constructions, both conformal and non-conformal, including the Sakai-Sugimoto model. These models obviously have an origin in a full-fledged string theory, however we will use them here without worrying about the validity of string theory approximations. Our attitude is pragmatic, in the sense that we are mainly interested in seeing how the models behave, with the eventual goal of improving the description of holographic superconductors and bringing them closer to real-world systems. For this reason, we will e.g. work with Yang-Mills action, without attempt to include DBI corrections to it, and we will also not consider gravitational back-reaction.

After an introduction to the models under consideration, we will first focus on their thermodynamic properties, in particular the specific heat. For all systems which we analyse, we find evidence that in the superconducting phase, they resemble non-BCS, heavy fermion compounds. That is, their specific heat has a polynomial behaviour as a function of temperature, in contrast to the exponential one seen in BCS superconductors. At a more quantitative level, we find that  $c_v \sim T^n$  where  $n \sim 2.7 - 5.5$  depending on the model. We also demonstrate the appearance of a jump in the specific heat at  $T_c$ , a property common to both strongly and weakly coupled superconductors. Above  $T_c$ , our approach only yields linear scaling for the specific heat at constant chemical potential for the D3/D7 system, while this is present also in the D4/D8 case in the DBI approximation [8]. The specific heat at constant density is, for all conformal cases, known to behave non-linearly [9].

We then continue in §4 with the analysis of electromagnetic properties. For most systems under consideration we find behaviour above the critical temperature which resembles that of a semi-conductor, i.e. a decreasing resistivity with increasing temperature. In the superconducting phase, there is a small region in temperature in which a condensate has already formed but the resistivity is not yet entirely zero. We find that the gap scales linearly with the critical temperature,  $\omega_g \propto T_c$ , but the proportionality constant is outside the BCS range and can also be substantially different from the ones found so far for conformal holographic superconductors.

In two sections (§3.3 and §4.3) we comment on the relation of our findings to real-world superconductors.

## 2. Colourful superconductors

### 2.1 Non-abelian condensates

Before we analyse a number of concrete holographic superconductors, let us first summarise the general setup and some universal aspects of the problem. We will consider generic diagonal metrics in which the time-time component of the line element is of the form  $-g(u) dt^2$ , where  $g(u)$  has a zero at the location of the horizon. An example of this sort is the metric of a  $Dp$ -brane, given by

$$ds_{Dp}^2 = \left(\frac{u}{L}\right)^{\frac{7-p}{2}} \left(-f_p(u) dt^2 + \delta_{ij} dx^i dx^j\right) + \left(\frac{u}{L}\right)^{\frac{p-7}{2}} \left(\frac{du^2}{f_p(u)} + u^2 d\Omega_{8-p}^2\right), \quad (2.1)$$

where  $i, j = 1 \dots p$  and  $f_p(u) = 1 - (u_T/u)^{7-p}$ . For our numerical analysis later in the paper it is advantageous to introduce coordinates in which the coordinate distance between the asymptotic boundary and the horizon is finite. We will use  $r := L^2/u$ . The  $Dp$ -brane metric then reads

$$ds_{Dp}^2 = \left(\frac{L}{r}\right)^{\frac{7-p}{2}} \left(-f_p(r) dt^2 + \delta_{ij} dx^i dx^j\right) + \left(\frac{L}{r}\right)^{\frac{p-7}{2}} \left(\frac{L^4 dr^2}{r^4 f_p(r)} + \frac{L^4}{r^2} d\Omega_{8-p}^2\right), \quad (2.2)$$

with  $f_p(r) = 1 - (r/r_T)^{7-p}$ . The horizon is now located at  $r = r_T$  and the asymptotic boundary is at  $r = 0$ . In this coordinate system the dilaton equals

$$e^{-\phi} = \left(\frac{L}{r}\right)^{(p-7)(p-3)/4}. \quad (2.3)$$

In addition to these  $Dp$ -brane systems we will also consider the  $AdS_4$  black hole background, with vanishing dilaton and metric given by

$$ds_{AdS_4}^2 = \left(\frac{L}{r}\right)^2 \left(-f_3(r) dt^2 + \delta_{ij} dx^i dx^j + \frac{dr^2}{f_3(r)}\right). \quad (2.4)$$

For future reference, we note here that the temperature of the  $Dp$ -brane backgrounds, as measured by an asymptotic observer following the orbit of the Killing vector  $\partial/\partial t$ , is given by

$$T = \frac{7-p}{4\pi L} \left(\frac{L}{r_T}\right)^{\frac{5-p}{2}}. \quad (2.5)$$

For the  $AdS_4$  black hole the temperature is  $T = 3/(4\pi r_T)$ .

If we now add a  $Dq$ -brane to the  $Dp$  brane background, the non-abelian gauge field on the  $Dq$ -brane can condense [6]; a similar story holds true when we add a Yang-Mills action to the  $AdS_4$  background [7]. We will here restrict attention to an  $SU(2)$  gauge field. The non-abelian condensate will occur if the chemical potential  $\mu$ , corresponding to the value of the  $A_0$  component on the boundary, is fixed to a large enough value. The system actually admits condensates of two different types [6, 7]. The one which generically turns out to have the largest energy of the two is of the form

$$A = A_0^{(3)} \sigma^3 dt + A(r) (\sigma^1 dx^1 + \sigma^2 dx^2). \quad (2.6)$$

This solution breaks the  $SU(2)$  symmetry to a diagonal  $U(1)$ . It is unstable [4], and expected to decay to a lower energy condensate. The lower energy configuration can be written in the form<sup>1</sup>

$$A = A_0^{(3)} \sigma^3 dt + A_3^{(1)} \sigma^1 dx^3. \quad (2.7)$$

Such a condensate is analogous to the one studied at zero temperature in [6], and we will return to this analogy in more detail in section 2.3. In the  $2 + 1$  dimensional case studied in [4], this condensate breaks both  $SU(2)$  and rotational invariance completely.

We will restrict ourselves to an analysis of the Yang-Mills truncation of the effective action on the probe brane (comments on the limitations of this approximation will be made in §3.2). The Lagrangian which determines the formation of a condensate of the type (2.7) is given by

$$L = -T_q \int_0^{r_T} dr \sqrt{-\hat{g}} e^{-\phi} \left[ \hat{g}^{00} \hat{g}^{rr} (\partial_r A_0^{(3)})^2 + \hat{g}^{33} \hat{g}^{rr} (\partial_r A_3^{(1)})^2 + 4 \hat{g}^{00} \hat{g}^{33} (A_0^{(3)} A_3^{(1)})^2 \right]. \quad (2.8)$$

This action leads to a coupled system of equations of motion,

$$\begin{aligned} \partial_r \left[ \sqrt{-\hat{g}} e^{-\phi} \hat{g}^{00} \hat{g}^{rr} \partial_r A_0^{(3)} \right] &= 4 (A_3^{(1)})^2 A_0^{(3)} \sqrt{-\hat{g}} e^{-\phi} \hat{g}^{00} \hat{g}^{33}, \\ \partial_r \left[ \sqrt{-\hat{g}} e^{-\phi} \hat{g}^{33} \hat{g}^{rr} \partial_r A_3^{(1)} \right] &= 4 (A_0^{(3)})^2 A_3^{(1)} \sqrt{-\hat{g}} e^{-\phi} \hat{g}^{00} \hat{g}^{33}, \end{aligned} \quad (2.9)$$

These are to be supplemented with boundary conditions at infinity, which take the form

$$A_0^{(3)} = \mu + \mathcal{O}(r), \quad A_3^{(1)} = \mathcal{O}(r). \quad (2.10)$$

and boundary conditions at the horizon, which follow from the requirement that  $A_0^{(3)}(r_T) = 0$ . One typically finds that for values of the chemical potential below a critical one,  $A_3^{(1)}$  is identically zero and the condensate is purely abelian. For chemical potentials larger than  $\mu = \mu_c$ , the  $A_3^{(1)}$  component turns on, making the condensate non-abelian. These solutions are parameterised by particular combinations of values of  $\partial_r A_0^{(3)}$  and  $A_3^{(1)}$  at the horizon. If one keeps increasing  $\mu$  substantially beyond the critical value, new branches of solutions occur. These typically have a larger energy and hence are expected to be unstable. An example of the structure of these solutions is given in figure 1.

## 2.2 Overview of the models

We will consider both three-dimensional and four-dimensional superconductors of the type described above. For the three-dimensional models we will focus on the  $AdS_4$  black hole and the non-conformal D2/D6 intersection.<sup>2</sup> Our main emphasis in the context of four-dimensional superconducting systems will be the one obtained from the Sakai-Sugimoto model [11]. However, in order to appreciate the variety of ways in which this model is a

---

<sup>1</sup>The use of the coordinate  $x^3$  is a bit misleading, and should *not* be understood to imply that this condensate only occurs in models which have at least three space dimensions.

<sup>2</sup>The non-abelian condensate in the  $AdS_4$  black hole background was previously constructed in [7]. The D2/D6 system allows, to some limited extent, an analysis which includes back-reaction effects [10], and it would be interesting to investigate how these influence the results obtained in the present section.

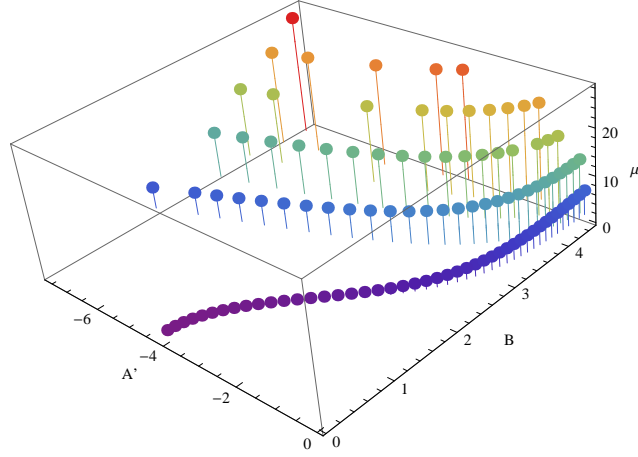


**Figure 1:** The structure of the condensate solution space for the D3/D7 system, showing the chemical potential  $\mu$  as a function of the two parameters  $A'$  and  $B$  which determine the solution at the horizon. Clearly visible are the various branches of condensates.

non-trivial superconductor, we will here also review some known facts about the D3/D7 superconductor, and extend them with several new results.

A Frobenius analysis of the equations near infinity reveals that the asymptotic behaviour of  $A_0^{(3)}$  and  $A_3^{(1)}$  is

$$\begin{aligned}
\text{AdS}_4 : \quad A_0^{(3)} &= \mu - \rho r + \dots, & A_3^{(1)} &= \mu' + \rho' r + \dots, \\
\text{D2/D6} : \quad A_0^{(3)} &= \mu - \rho r^2 + \dots, & A_3^{(1)} &= \mu' + \rho' r^2 + \dots, \\
\text{D3/D7} : \quad A_0^{(3)} &= \mu - \rho r^2 + \dots, & A_3^{(1)} &= \mu' + \rho' r^2 + \dots, \\
\text{D4/D8} : \quad A_0^{(3)} &= \mu - \rho r^{3/2} + \dots, & A_3^{(1)} &= \mu' + \rho' r^{3/2} + \dots.
\end{aligned} \tag{2.11}$$

In all of the cases we will be interested in solutions for which the chemical potential for  $A_0^{(3)}$  is turned on, while it is set to zero for  $A_3^{(1)}$ ; in other words we are looking for solutions which satisfy the boundary conditions  $\mu \neq 0$  and  $\mu' = 0$ . As usual we also require that, for regularity of the solution, at the horizon  $A_0^{(3)}(r_T) = 0$ . The equations of motion then imply that the near-horizon behaviour of the fields is (for all cases)

$$A_0^{(3)} = A'(r - r_T) + \dots, \quad A_3^{(1)} = B + \dots. \tag{2.12}$$

By performing a two-dimensional scan through the parameter space spanned by  $A'$  and  $B$  and selecting those values for which the solutions to (2.9) satisfy the boundary condition that  $\mu' = 0$ , we arrive at the condensate solutions.

It is convenient to express these solutions in terms of a dimensionless condensate  $\hat{\rho}$ ,

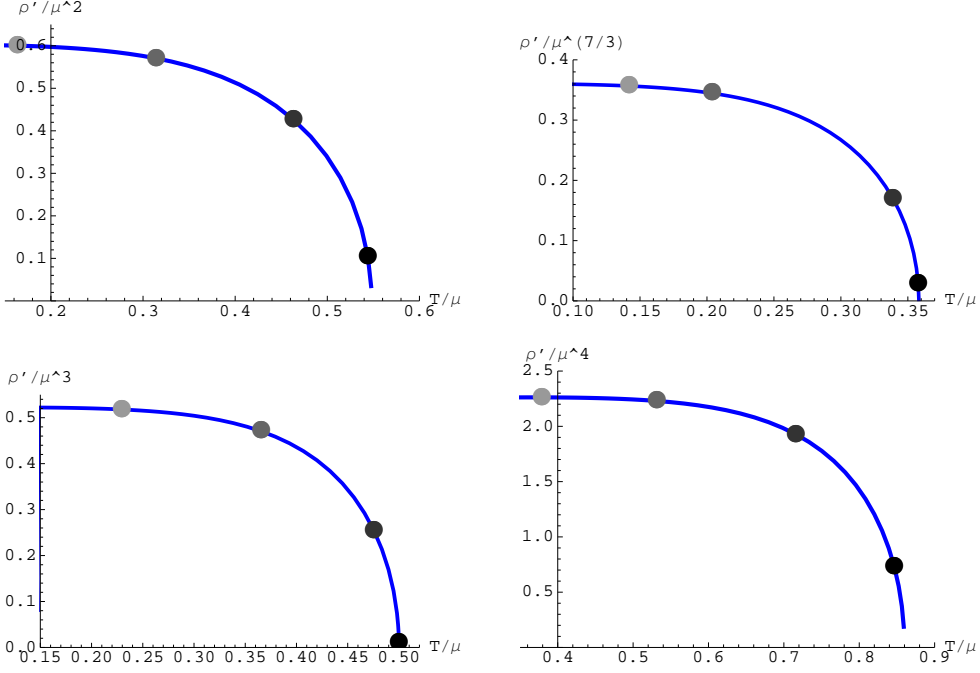


**Figure 2:** The dimensionless condensates  $\hat{\rho}'$  for (left to right, top to bottom) the  $\text{AdS}_4$  black hole, D2/D6, D3/D7 and D4/D8 systems, as a function of the dimensionless ratio  $T/\mu$  (or to be numerically precise,  $r_T^{(p-5)/2}/\mu$ ). The dots indicate selected states for which further properties will be analysed in section 4.

given for the various systems by

$$\begin{aligned}
\text{AdS}_4 : \quad \hat{\rho} &= \rho/\mu^2, \\
\text{D2/D6} : \quad \hat{\rho} &= \rho/\mu^{7/3}, \\
\text{D3/D7} : \quad \hat{\rho} &= \rho/\mu^3, \\
\text{D4/D8} : \quad \hat{\rho} &= \rho/\mu^4,
\end{aligned} \tag{2.13}$$

(similar expressions hold for  $\rho'$ ). The advantage of using  $\hat{\rho}$  and  $\hat{\rho}'$  is that these only depend on one dimensionless quantity  $\mu/T$ , not on the product  $TL$  (see appendix A for more details).

Plots of the dimensionless condensate  $\hat{\rho}'$  versus the ratio  $T/\mu$  are given in figure 2. We see that at fixed temperature the condensate is nonvanishing when  $\mu \leq \mu_c$ , while  $\hat{\rho}' = 0$  for  $\mu > \mu_c$ . In other words, the system undergoes a second-order phase transition as the chemical potential is changed. By numerically fitting the curves we see that the critical coefficient  $\alpha$ , which determines the scaling behaviour of the condensate in the vicinity of the critical point according to  $\hat{\rho} \sim (T/\mu_c - T/\mu)^\alpha$ , is  $\alpha = 1/2$ , in agreement with Landau-Ginzburg theory.

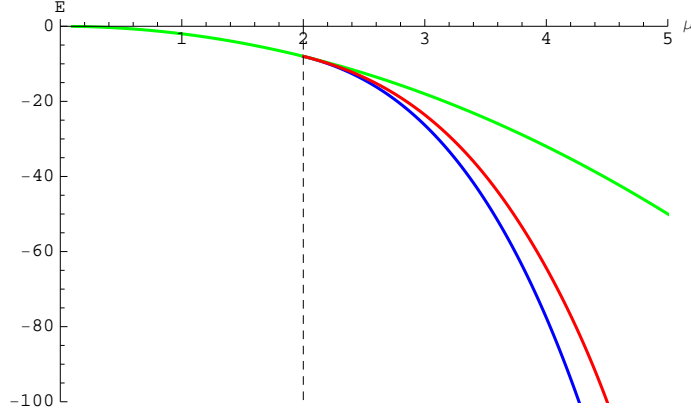


**Figure 3:** Comparison of the energy of the two non-abelian condensates and the abelian one, for the D3/D7 system, as a function of the chemical potential. The “three-component condensate” (2.6) (middle curve) always has a larger energy than the “two-component condensate” (2.7) (lower curve), and both have, for  $\mu > \mu_c \approx 2.0$ , a lower energy than the abelian one (upper curve). The other systems analysed in this paper exhibit similar behaviour.

For the alternative condensate given in (2.6), which is governed by the equations

$$\begin{aligned} \partial_r \left[ \sqrt{-\hat{g}} e^{-\phi} \hat{g}^{00} \hat{g}^{rr} \partial_r A_0^{(3)} \right] &= 8 A^2 A_0^{(3)} \sqrt{-\hat{g}} \hat{g}^{00} \hat{g}^{33} e^{-\phi}, \\ \partial_r \left[ \sqrt{-\hat{g}} e^{-\phi} \hat{g}^{33} \hat{g}^{rr} \partial_r A \right] &= 4 \left[ (A_0^{(3)})^2 \hat{g}^{00} - A^2 \hat{g}^{33} \right] A \sqrt{-\hat{g}} \hat{g}^{33} e^{-\phi}, \end{aligned} \quad (2.14)$$

the density as a function of the inverse chemical potential behaves similarly. However, the energy of this configuration, obtained by evaluating  $E = -L$  with  $L$  given by (2.8) is consistently higher. A comparison is displayed in figure 3. We will henceforth restrict ourselves to the lowest-energy condensate, which is the true ground state of the model.

### 2.3 Comments on the zero temperature limit

The strict zero temperature limit of holographic superconductors remains somewhat of a mystery. In principle, there are three different scenarios. In the first one, one takes a naive zero temperature limit of the black hole metric, and obtains a metric with a Poincaré horizon. This is what happens in the D3/D7 system upon taking  $r_T \rightarrow 0$ . The resulting system suffers from the fact that a condensate now becomes singular, even when using the full DBI action.

Another possibility is that the limit should be taken in such a way that an extremal horizon is obtained. Concrete examples of this type have not yet been found, but they would presumably avoid the triviality of the Poincaré horizon case discussed above. An attempt to analyse the zero-temperature situation was made in [12] by constructing a solution interpolating between two different  $\text{AdS}_4$  metrics. However, because of the conformal symmetry in the infrared, the solution found there exhibits a power-law scaling of the conductivity for small frequency, and hence no gap [13].



There remains one further option, which seems more natural in e.g. the Sakai-Sugimoto model. In contrast to e.g. the AdS<sub>4</sub> black holes used in many studies of holographic superconductors, the Sakai-Sugimoto model has a well-understood limit to zero temperature. For sufficiently low temperature, the system undergoes a first order phase transition [14]. One then obtains a D4/D8 system in which there is no horizon on the brane, and the D8-branes which were previously intersecting the horizon are now connected in a smooth way. This system admits non-abelian condensates (as analysed in [6]). The absence of a horizon automatically implies that there is no dissipation in the system.

### 3. Thermodynamic properties

#### 3.1 Free energy and specific heat

Let us now turn to an analysis of some of the thermodynamic properties of the superconductors. We will first present the results for the holographic models and then we will compare these with real world superconductors in section 3.3.

There has been some confusion in the literature as to the parameters which should be kept fixed when computing the specific heat. From the point of view of an experimental setup, keeping the density  $\rho$  constant is the most natural. This type of computation has been done for the abelian condensate of the D3/D7 case, using a full DBI analysis, in [9]. Alternatively, one could consider keeping the chemical potential  $\mu$  constant, which is a natural thing to do from the point of view of some holographic setups. A computation of this type can be found in e.g. [8]. Depending on what is kept fixed, the results can be quite different in as far as the dependence on the temperature is concerned. We will here elucidate these differences and then continue to show how the results change when one considers a non-abelian condensate instead.

The main technical ingredient in the computation of the temperature dependence of the free energy is the scaling symmetry discussed in section A. It allows us to study the temperature dependence by analysing the dependence on the chemical potential  $\mu$  at fixed temperature. By writing the Euclidean action in dimensionless coordinates and dimensionless fields  $\tilde{A}_0$  and  $\tilde{A}_3$ , we find that

$$\begin{aligned}
\text{AdS}_4 : \quad S_E(T) &= (TL)^2 \times \tilde{S}_E(\mu/T), \\
\text{D2/D6} : \quad S_E(T) &= (TL)^{\frac{7}{3}} \times \tilde{S}_E(\mu/T), \\
\text{D3/D7} : \quad S_E(T) &= (TL)^3 \times \tilde{S}_E(\mu/T), \\
\text{D4/D8} : \quad S_E(T) &= (TL)^4 \times \tilde{S}_E(\mu/T),
\end{aligned} \tag{3.1}$$

In writing these factors we have taken into account that the integral over the Euclidean time circle produces a factor of  $1/T$ .

For the computation of the heat capacity we now use the free energy  $F = TS_E$  together with

$$c_v = T \frac{\partial s}{\partial T} \quad \text{with} \quad s = -\frac{\partial F}{\partial T}, \tag{3.2}$$

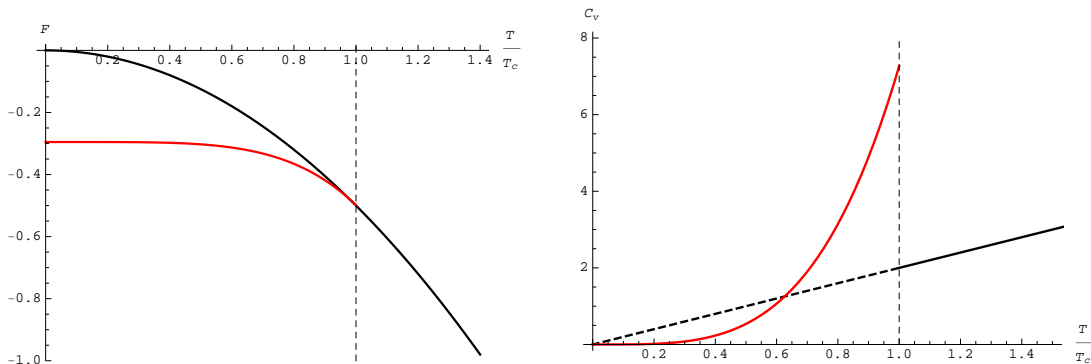


**Figure 4:** Free energies and specific heat for the D3/D7 system, as a function of temperature, for fixed chemical potential  $\mu$  (and hence with  $\rho = \rho(T)$ ). The black curve denotes the abelian condensate with only  $A_0$  non-zero, while the red curve denotes the non-abelian condensate.

where  $s$  is the entropy density, and we have suppressed volume factors. Using the form (3.1) it is easy to compute quantities like the free energy or the specific heat at fixed chemical potential  $\mu$ . In order to compute at fixed density  $\rho$ , one has to express  $\mu/T$  in terms of  $\hat{\rho}$  using condensate curves like those of figure 2.

Figure 4 shows curves for the free energy  $F(T)$  at constant  $\mu$ ; the curves at constant  $\rho$  are qualitatively similar. After normalising  $F(T=0) = 0$ , a double-logarithmic plot (not shown here) leads to practically straight curves, which suggests a fit of the free energy to a function of the form  $a + bT^c$  (as opposed to something involving exponentials of the temperature). We will comment below on how this connects to real-world superconductors. From the fit of the free energy we then obtain  $c_v$  by applying (3.2) to the fit, and arrive at the following numerical estimates in the normal and superconducting phases<sup>3</sup>,

	normal phase	superconducting	
	$c_v(\mu = \text{ct.})$	$c_v(\mu = \text{ct.})$	$c_v(\rho = \text{ct.})$
AdS <sub>4</sub> :	$T^0$	$T^{2.7}$	$T^{2.9}$
D2/D6:	$T^{\frac{1}{3}}$	$T^{3.0}$	$T^{3.2}$
D3/D7:	$T$	$T^{3.8}$	$T^{3.9}$
D4/D8:	$T^2$	$T^{5.5}$	$T^{5.2}$

(3.3)

As explained below, the results for the free energy in the abelian phase at constant  $\rho$  are unreliable in the Yang-Mills truncation, and we have therefore not indicated values for  $c_v(\rho = \text{const.})$  in the normal phase. The systematic error bars on the numerical exponents receive contributions from various stages of the construction and should thus only be used as indicators about the numbers of degrees of freedom.

The only previous result about the specific heat of a non-abelian condensate is, as far as we are aware, given in the work of [15]. These authors claim that  $c_v(\rho = \text{const.}) \sim T^3$  for the

<sup>3</sup>Numerically it is more reliable to fit  $F$  rather than  $c_v$ . The ansatz is consistent with the fact that  $c_v$  should vanish as  $T \rightarrow 0$ , as required by the third law of thermodynamics.

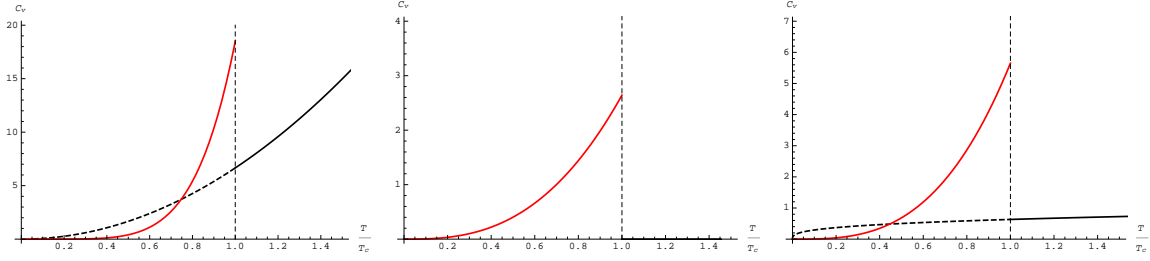


**Figure 5:** Specific heat for the D4/D8, AdS<sub>4</sub> and D2/D6 systems respectively; curves as in figure 4. The free energy plots of these systems are similar to figure 4a, the only difference being the exponents of the curves.

D3/D7 system (analysed using the non-abelian DBI action in two different prescriptions). Our computations for D3/D7 lead to a somewhat larger exponent: they also contain a factor  $T^3$ , arising from the overall prefactor in (3.1), but we find an additional temperature dependence through  $\tilde{S}(\mu/T)$ . This difference may be a consequence of the DBI corrections to the Yang-Mills action, but we did not check the results of [15].

The most important conclusion to draw from our analysis – more important than the actual numbers – is the fact that we find no evidence for exponential suppression of the specific heat in the superconducting phase. As we will see, this is in sharp contrast with BCS-like superconductors. The second important result is that the non-abelian systems exhibit a jump in the specific heat at the phase transition. We will discuss the relevance of these findings to real world superconductors in §3.3.

### 3.2 Limitations of the Yang-Mills approximation

The result for the specific heat at constant *density* for the abelian condensate (i.e. above  $T_c$ ), which were obtained from our Yang-Mills analysis, differ substantially from the ones obtained using a DBI analysis [9]. However, we have also seen that computing the specific heat above  $T_c$  at constant *chemical potential*, gives a much better agreement with the DBI computation [8]. The reason for this seems directly related to the behaviour of the corresponding two gauge field solutions in the zero-temperature limit, as the one at constant chemical potential admits a smooth  $T \rightarrow 0$  limit while the solution at fixed density does not.

To see this explicitly, consider the abelian solution to the Yang-Mills equations of motion, for instance for the D4/D8 model. It reads

$$\partial_r A_0 = \rho r^{1/2}. \quad (3.4)$$

The chemical potential and the free energy are (making use of (2.5), i.e.  $T = 3/(4\pi\sqrt{rT})$ )

$$\begin{aligned} \mu &= \int_0^{rT} \partial_r A_0 = \int_0^{rT} dr \rho r^{1/2} = \frac{2}{3} \rho \left( \frac{4}{3} \pi T \right)^{-3}, \\ F &= \int_0^{rT} \sqrt{-g} e^{-\phi} g^{rr} g^{00} (\partial_r A_0)^2 = \int_0^{rT} dr \rho^2 r^{1/2} = \rho \mu. \end{aligned} \quad (3.5)$$

The latter expression yields  $\partial F/\partial\mu = \rho$ , confirming that  $\rho$  is the density. Clearly, if we keep  $\rho$  fixed and take the limit  $T \rightarrow 0$ , the gauge field becomes singular at the horizon  $r = r_T$ . However, if we eliminate  $\rho$  in favour of  $\mu$ , then the gauge field becomes  $\partial_r A_0 = \frac{3}{2}\mu \left(\frac{4}{3}\pi T\right)^3 r^{1/2}$ . At  $r = r_T$  this is regular for  $T \rightarrow 0$ . A similar analysis holds for the other models analysed in this paper. In contrast, the non-abelian solutions always seem to be regular in the  $T \rightarrow 0$  limit.

### 3.3 Comments on connections with real-world superconductors

Knowledge of the specific heat in solid state physics is of central importance, as it shows what are the relevant degrees of freedom, and how these vary with temperature. In addition, this quantity is in a sense “simpler” and more robust than e.g. the resistivity, since, as a scalar quantity, it is insensitive to the anisotropic properties of the material. For standard metals the specific heat  $c_v$  behaves as

$$c_v \equiv c_v^{\text{el}} + c_v^{\text{ph}} = \gamma T + \beta T^3. \quad (3.6)$$

The first term, proportional to the Sommerfeld constant  $\gamma$ , originates from an electronic contribution and the second term originates from lattice phonons. While the lattice contribution to the specific heat is unchanged for superconductors, the electronic part varies significantly, depending on the type of superconductor (see e.g. [16]).

The weakly coupled superconductors are successfully described with BCS theory, which predicts that the specific heat is exponentially suppressed for temperatures  $T < T_c$ , i.e.

$$\frac{c_v}{\gamma T_c} = A e^{-B \frac{T_c}{T}}. \quad (3.7)$$

Here  $\gamma$  is the Sommerfeld constant in the normal phase, and  $A$  and  $B$  are constants that depend on the temperature interval. Therefore, for sufficiently low temperatures the graph  $\ln(C/\gamma T_c)$  against  $T_c/T$  is a straight line, which is also experimentally observed (see the left panel of figure 6). The exponential suppression of the specific heat is a natural consequence of the presence of a gap, since when  $T < T_c/2$ , the energy necessary to break a Cooper pair is  $\sim 2\Delta(0)$ , and the number of broken pairs is  $\sim e^{-2\Delta(0)/k_B T}$ . Another important feature of low  $T_c$  superconductors is that the specific heat is *discontinuous* at  $T = T_c$  since at this temperature it is no longer necessary to put energy into breaking of Cooper pairs. BCS theory predicts a universal number for this jump,  $\Delta c(T_c)/\gamma T_c = 1.43$ , which is indeed observed in a large number of low- $T_c$  superconductors.

Another class of superconductors are the *strongly coupled* superconductors which include for example high- $T_c$  superconductors and heavy fermion compounds. Most of these materials are experimentally found to involve higher-spin electric carriers. From this perspective one might expect that these materials should be more similar to non-abelian (spin one) condensates considered in this paper. Heavy fermion compounds are very different from BCS-like materials when cooled down to the superconducting phase. They have a specific heat below  $T_c$  which is well-approximated with a power law behaviour (see e.g. [19]),

$$\text{heavy fermions at } T < T_c : \quad c_v = \gamma_0 T + \kappa T^n, \quad (3.8)$$

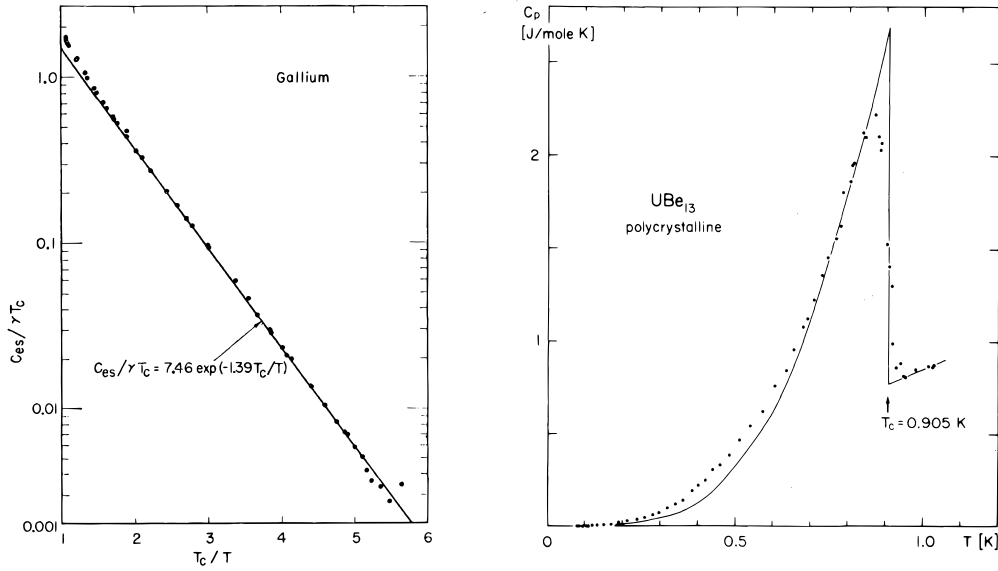


**Figure 6:** Specific heat of the low- $T_c$  BCS superconductor gallium (left) and the heavy-fermion compound  $\text{UBe}_{13}$  (right) in their superconducting phases. Figures taken from [17] and [18] respectively.

where  $n \sim 2-3$ , and  $\gamma_0$  and  $\kappa$  are constants. In other words, due to the unusual properties of the gap, the specific heat is no longer exponentially suppressed when  $T < T_c$ . The specific heat jump at  $T = T_c$ , which is observed for the weakly coupled materials, does exist for the strongly coupled superconductors as well, although the normalised value of the jump is, for many systems, much larger than the value 1.43 predicted by BCS theory (see the right panel of figure 6).

When heated above  $T = T_c$ , a large number of heavy fermion compounds behave as a (heavy) fermion liquid, i.e. with specific heat  $c/T \sim \gamma(T) = \text{const.}$ . However, some of them (for example  $\text{UBe}_{13}$ ) have an unusual behaviour and their specific heat is well-described by

$$\text{heavy fermions at } T > T_c : \quad c_v \sim \frac{T}{T_0} \ln \left( \frac{T_0}{T} \right) \quad \text{or} \quad c_v \sim T^\lambda \quad (\lambda \approx 0.7 - 0.8). \quad (3.9)$$

Keeping all this in mind we can try to compare some of our findings with real superconductors. Firstly, we see that in the superconducting phase, colourful holographic superconductors have power-law behaviour of the specific heat, which is closer to the strongly coupled superconductors, not the BCS superconductors. Secondly, all systems exhibit a jump in the specific heat, in agreement with real-world superconductors.

Finally, when  $T > T_c$ , in all cases the specific heat *increases* with temperature according to a power law. The precise value of the positive exponents depends on details of the system, on whether we work at fixed chemical potential or at fixed density (see the previous section), and finally it depends on whether we work in the Yang-Mills approximation (see table 3.3) or with the full DBI action [9]. From the experimental perspective the specific heat at fixed  $\rho$  is a more interesting quantity, and as we have already explained the

Yang-Mills approximation is in this case not appropriate. To analyse the  $T > T_c$  temperature range, we thus use the results of [9]. All cases considered in [9] are conformal, such that the non-sphere part of the D-brane worldvolume is  $\text{AdS}_{p+2}$ . They find that  $c \sim T^{2p}$ . Hence none of the conformal cases seem to fit the metallic behaviour of heavy fermion compounds. The specific heat at fixed  $\mu$  seems more close to real-world superconductors, since in the Yang-Mills approximation the D2/D6 system has exponent 1/3, resembling (3.9) and D3/D7 has metallic behaviour, while in the DBI approximation the D4/D8 system exhibits metallic behaviour [8].

In summary, from the perspective of the specific heat, most of the colourful holographic superconductors show some qualitative similarities with strongly coupled superconductors. In particular, modulo subtleties discussed above, the D3/D7 system looks very similar to e.g. the  $\text{UBe}_{13}$  heavy fermion superconductor.

## 4. Electromagnetic properties

In this section we turn to a study of the response functions for the superconducting condensates that were constructed in the previous sections. In particular, we focus on the computations of AC and DC conductivities. At the end we compare our holographic findings with qualitative features of real-world superconductors.

### 4.1 AC conductivity

Once a condensate has been found, response functions in this background can be obtained by analysing the Green function of the gauge field fluctuations. For the condensate (2.7), one can in principle fluctuate in the direction parallel to the condensate or orthogonal to it [4]. Here we choose to consider only fluctuations orthogonal to the condensate, i.e. we look at the fluctuation modes in the  $\psi \equiv A_2^{(3)}$  field. These fluctuation modes satisfy

$$\partial_r \left[ \sqrt{-\hat{g}} e^{-\phi} \hat{g}^{rr} \hat{g}^{22} \partial_r \psi \right] - 4 \sqrt{-\hat{g}} e^{-\phi} \hat{g}^{33} \hat{g}^{22} (A_3^{(1)})^2 \psi - \sqrt{-\hat{g}} e^{-\phi} \hat{g}^{00} \hat{g}^{22} \omega^2 \psi = 0. \quad (4.1)$$

In particular, the Green function is obtained from the boundary data using

$$G_R(\omega) = - \lim_{r \rightarrow 0} \sqrt{-\hat{g}} e^{-\phi} \hat{g}^{33} \hat{g}^{rr} \psi \partial_r \psi. \quad (4.2)$$

and the AC conductivity then follows from

$$\sigma(\omega) = \frac{G_R(\omega)}{i\omega}. \quad (4.3)$$

The fluctuation equation (4.1) exhibits properties just like the condensate equations. Following an analysis similar to that for condensate equations (see the appendix), we put it in the form

$$\partial_{\tilde{r}} \left( h_3(\tilde{r}) \partial_{\tilde{r}} \psi \right) - \left[ 4(A_3^{(1)})^2 h_5(\tilde{r}) + \omega^2 h_2(\tilde{r}) \right] T^{-2} \psi = 0. \quad (4.4)$$

From this we conclude that the conductivity  $\sigma$  will be a function of the two dimensionless parameters  $\tilde{\mu}$  and  $\hat{\rho}(\tilde{\mu})$  which appear in (A.2), as well as the combination  $\omega/T$ .

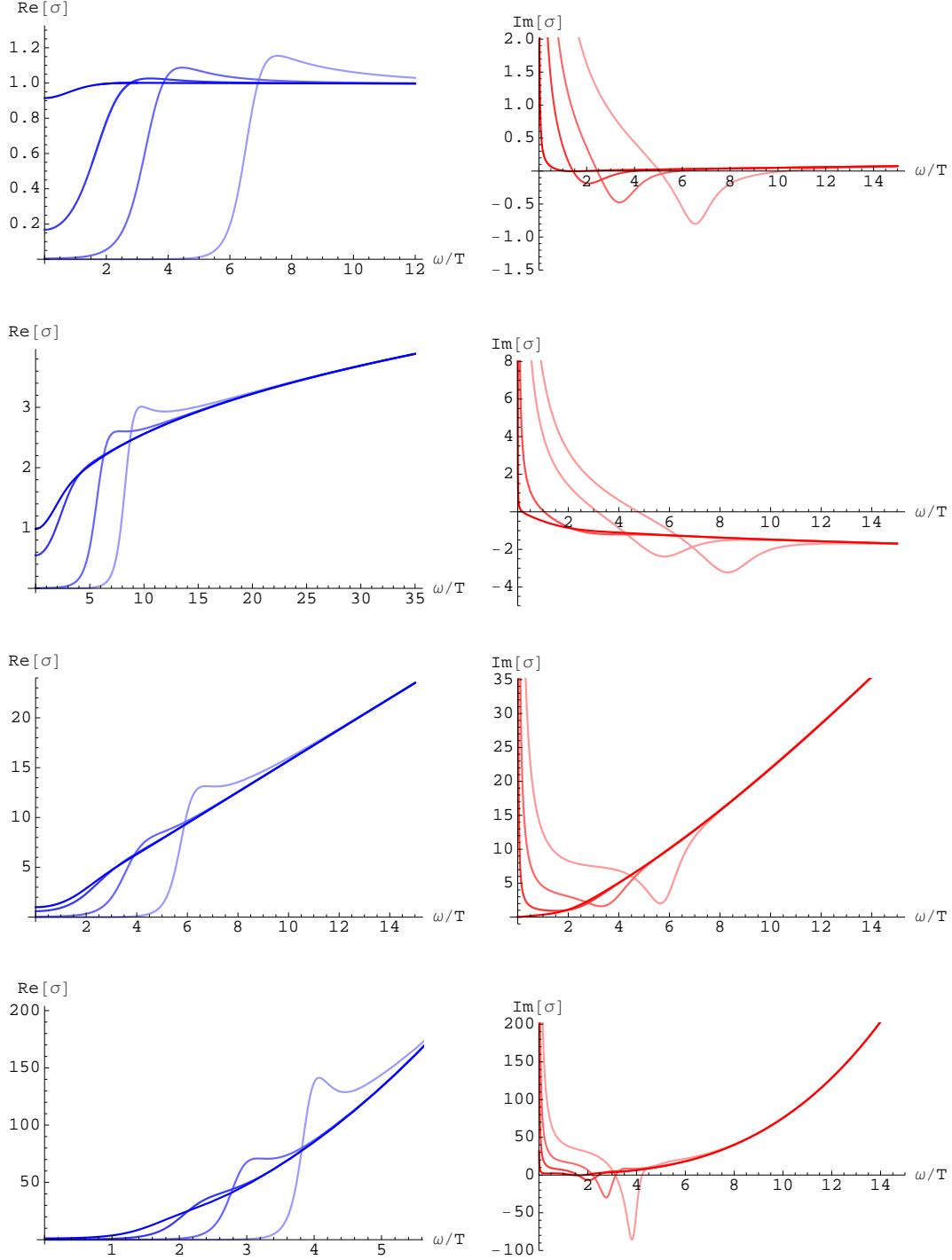


**Figure 7:** Real and imaginary parts of the conductivity for the four systems (from top to bottom:  $\text{AdS}_4$ , D2/D6, D3/D7 and D4/D8), plotted for various values of the dimensionless chemical potential  $\mu/T$  (corresponding to the dots in figure 2).

In the D3/D7 case, computing the conductivity requires some extra care because of the presence of logarithmic terms in the asymptotic expansion of the gauge field fluctuations [20, 21]. A perturbative analysis yields

$$\psi = a_0 \left( 1 - \frac{1}{2} \omega^2 r^2 \log(\Lambda r) + \dots \right) + a_2 r^2 + \dots \quad (4.5)$$

When evaluating the conductivity (4.3) this leads to a logarithmically divergent term as well as a finite contribution.<sup>4</sup> The logarithmically divergent term can be removed by suitable addition of a holographic counterterm.

We impose ingoing boundary condition on the fluctuation  $\psi$  at the horizon, which means

$$\psi = (r_T - r)^{-i\alpha\omega} (1 + a_1(r_T - r) + a_2(r_T - r)^2 + \dots) \quad \text{near } r = r_T, \quad (4.6)$$

where  $\alpha$  is a model-dependent real coefficient,  $\frac{1}{3}r_T$ ,  $\frac{1}{5}r_T^{3/2}$ ,  $\frac{1}{4}r_T$ , and  $\frac{1}{3}\sqrt{r_T}$  for the AdS<sub>4</sub>, D2/D6, D3/D7 and D4/D8 models respectively. After shooting to the boundary at  $r = 0$  we then compute the retarded Green function from (4.2). We have analysed the real and imaginary parts of the conductivity for all four systems; the results are displayed in figure 7.

There is a number of interesting features in both the three and four-dimensional cases. First, in comparison to holographic superconductors obtained from AdS<sub>4</sub> black holes in four-dimensional Abelian Higgs models, such as analysed in [21], we see that for all other cases, in the absence of a condensate, the real part of the conductivity does not approach a constant. This is in particular true for the two-dimensional, non-conformal D2/D6 system. Second, we see that the value of the chemical potential where a gap in the real part of the conductivity appears, does not coincide with the critical value of  $\mu$  where the condensate forms. The gap forms at a *larger* value of  $\mu$ , and becomes more pronounced as  $\mu$  increases.

In all cases we have analysed, there is a strong evidence for the scaling of the energy gap with the critical temperature,

$$\frac{w_g}{T_c} \approx \text{constant}. \quad (4.7)$$

This is most easily seen from the plots of the conductivity versus the dimensionless ratio  $\omega/\mu$ ; an example is given in figure 8 for the D4D8 system. Following [21], we define  $\omega_g$  as the frequency for which  $\text{Im } \sigma$  has a minimum (following [21]). The relation between the critical temperature  $T_c$  and the chemical potential  $\mu$  is read off from the plots of the condensate versus  $T/\mu$  in figure 2: the intersection of these curves with the horizontal axis yields the value of  $T/\mu$  for which the condensate first appears, and hence gives  $T_c$  for a

---

<sup>4</sup>An analysis of the non-abelian condensate in the D3/D7 system has previously appeared in [22] but that paper ignores the effect of the logarithmic terms in the fluctuation, as witnessed by e.g. the different imaginary part of the conductivity.



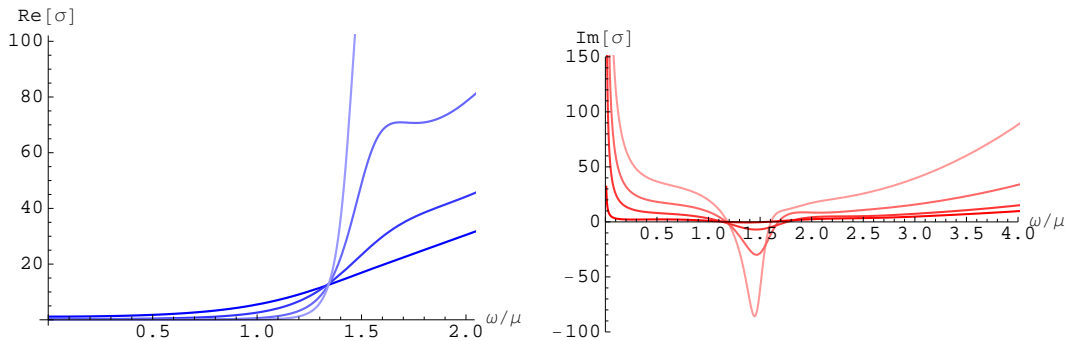


**Figure 8:** The real and imaginary part of the conductivity of the D4/D8 system, versus the dimensionless ratio  $\omega/\mu$ , for various values of  $\mu/T$  (corresponding to the dots in figure 2). If we define  $\omega_g$  to be the frequency for which the imaginary part of the conductivity has its minimum, this plot shows that  $\omega_g \sim \mu$ . The other systems show qualitatively similar behaviour.

given  $\mu$ .<sup>5</sup> In this way we obtain

$$\begin{aligned}
\text{AdS}_4 : \quad T_c/\mu &\approx 0.13, & \omega_g/T_c &\approx 8.4, \\
\text{D2/D6} : \quad T_c/\mu &\approx 0.14, & \omega_g/T_c &\approx 8.0, \\
\text{D3/D7} : \quad T_c/\mu &\approx 0.16, & \omega_g/T_c &\approx 8.1, \\
\text{D4/D8} : \quad T_c/\mu &\approx 0.21, & \omega_g/T_c &\approx 6.7.
\end{aligned} \tag{4.8}$$

In the conformal cases analysed thus far this ratio turned out to be around 8 to within a few percent. This is in contrast to the BCS values which are anywhere between 3.5 at weak coupling and 4 in the naive strong coupling limit (see e.g. [23]). The non-conformal cases give results which are higher than the BCS result too, with the D4/D8 value deviating substantially from 8. Our results for the non-abelian condensate in the  $\text{AdS}_4$  black hole background is similar to the one for the  $\text{AdS}_4$  Abelian Higgs model of [21].

One final way to compare the holographic superconductors with experimental data on superconductors is to express the results in terms of the real resistivity, defined as

$$R = \frac{\text{Re } \sigma}{(\text{Re } \sigma)^2 + (\text{Im } \sigma)^2}. \tag{4.9}$$

Although plots of  $R$  versus  $\omega$  for the AC behaviour are not very common in the literature, we have provided these for completeness in figures 9. We will have more comments on the behaviour of the DC resistivity in the next section.

## 4.2 DC conductivity

It has recently been noted that the  $\omega = 0$  limit of the real part of the conductivity can be expressed in terms of quantities at the horizon, rather than at infinity [24]. By expressing

<sup>5</sup>In reading off the numerical coefficient, it should be noted that the variable along the horizontal axes of these plots is  $qT/\mu$ , with the proportionality constant  $q$  chosen such that this reduces to  $1/\mu$  when  $r_T = L = 1$ .

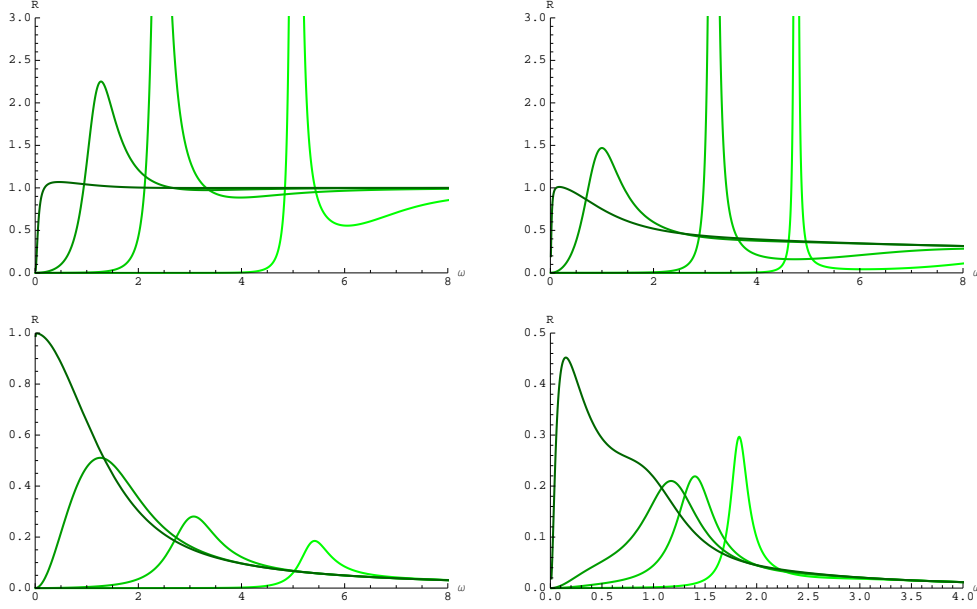


**Figure 9:** Resistivity as a function of frequency (left to right, top to bottom:  $\text{AdS}_4$ ,  $\text{D2/D6}$ ,  $\text{D3/D7}$  and  $\text{D4/D8}$ ), for various values of  $\mu/T$  (corresponding to the dots in figure 2). Lighter curves correspond to larger chemical potential.

the conductivity in terms of the canonical momentum, and noting that it satisfies a trivial flow equation in the radial direction. The conductivity can be expressed in terms of a quantity evaluated at the horizon. A generalisation of their argument to include a dilaton reads

$$\text{Re } \sigma_{\text{DC}} \propto \sqrt{\frac{-g}{g_{rr}g_{tt}}} g^{xx} e^{-\phi} \Big|_{r=r_t}, \quad (4.10)$$

(where the proportionality involves an overall coupling constant dependence which will not be important here). For the cases analysed here, this expression yields  $\text{Re } \sigma \propto 1$ ,  $T^{1/3}$ ,  $T$  and  $T^2$  respectively<sup>6</sup>. It is important to note that, except for the conformal  $\text{AdS}_4$  case, these are all increasing functions of temperature, quite in contrast to e.g. ordinary metals. We should also note that while the result of [24] was derived in the absence of any condensate, it is also relevant for the abelian condensate, since in the Yang-Mills approximation the fluctuation equations decouple from the abelian condensate.

This behaviour of the DC conductivity at zero condensate is indeed easily verified to hold true for our numerical results in the  $\omega \rightarrow 0$  limit, thus providing a quick test of our analysis in the abelian case. In fact, one can again use the properties of equation (4.4) explained in the appendix to analyse the behaviour of  $\sigma$  as a function of  $T$ . First, one notes that in  $\tilde{r}$  coordinates the Green function (4.2) is given by an overall power of  $TL$

---

<sup>6</sup>The  $\text{D3/D7}$  behaviour agrees with [25] and is the same as found for the Abelian Higgs model in [21].

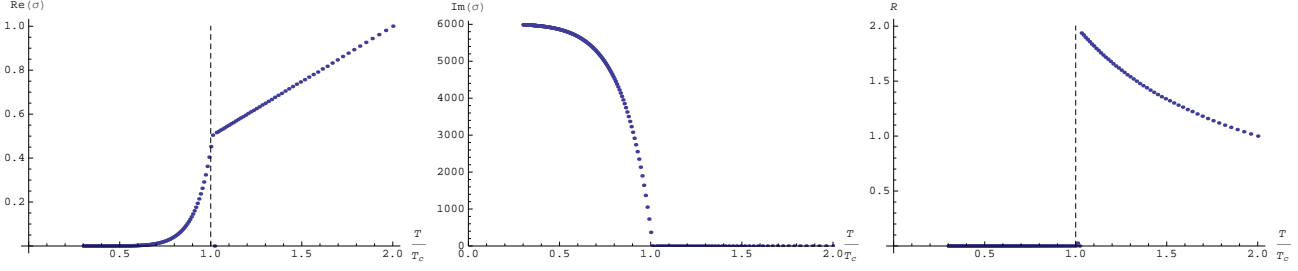


**Figure 10:** The real and imaginary part of the DC conductivity (or rather, the AC conductivity at fixed small frequency) as a function of temperature, and the resistivity, for the D3/D7 system. For temperatures  $T > T_c$  the condensate becomes abelian and we recover the  $\text{Re } \sigma \propto T$  result of [24, 25], which is the large-temperature limit of [20]. For  $T < T_c$  there is a regime for which  $\text{Re } \sigma$  is not yet zero, but shows a polynomial dependence on the temperature.

multiplied with a function of  $\omega/T$ . These factors of  $TL$  are

$$\begin{aligned}
 \text{AdS}_4 : \quad G_R(\omega, T) &= (TL) \times \tilde{G}_R(\omega/T, \mu/T), \\
 \text{D2/D6} : \quad G_R(\omega, T) &= (TL)^{\frac{4}{3}} \times \tilde{G}_R(\omega/T, \mu/T), \\
 \text{D3/D7} : \quad G_R(\omega, T) &= (TL)^2 \times \tilde{G}_R(\omega/T, \mu/T), \\
 \text{D4/D8} : \quad G_R(\omega, T) &= (TL)^3 \times \tilde{G}_R(\omega/T, \mu/T).
 \end{aligned} \tag{4.11}$$

The only bare  $\omega$  dependence enters through the denominator of (4.3).

Once the non-abelian condensate is turned on, the analysis of [24] can no longer be applied. The coupling between the fluctuation and the gauge field component  $A_x$  implies that it is now no longer true that the radial evolution of the canonical momentum is trivial. Hence it is no longer possible to express the conductivity in terms of a quantity evaluated at the horizon. Nevertheless, it is possible to analyse the temperature dependence of the conductivity in the  $\omega \rightarrow 0$  limit numerically. The scaling properties imply that  $\mu/T \propto \omega/T$ . Figure 10 displays the behaviour of the conductivity and resistivity in this non-abelian phase.<sup>7</sup>

Generically, we see that superconductors of the holographic type exhibit a behaviour of the resistivity which is similar to that of semi-conductors, i.e.  $R$  decreases with temperature above the critical temperature. A metallic behaviour has so far only been found for small temperatures in the model of [20].

#### 4.3 Comments on connections with real-world superconductors

We have already seen in section 3.3 that weakly coupled and strongly coupled superconductors exhibit very different behaviour for their specific heat. As far as the electric resistivity of these materials is concerned, while all of them have zero resistivity for  $T < T_c$ , when

<sup>7</sup>The metallic  $\text{Re } \sigma \propto 1/T^2$  behaviour at small temperatures, found in [20], is invisible in the Yang-Mills truncation. It is, however, unclear whether it will show up before the transition to the non-abelian condensate takes place.

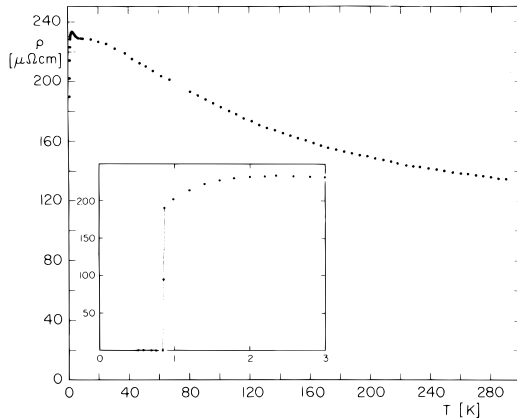


**Figure 11:** Resistivity of the heavy fermion compound  $\text{UBe}_{13}$ . Figure taken from [26].

$T > T_c$ , their behaviour again differs significantly. The weakly coupled superconductors mainly behave as “metals” above  $T_c$  (i.e. with a resistivity that grows with  $T$  as a polynomial of  $T$ ). On the other hand, just above  $T_c$  strongly coupled superconductors behave either as metals or as semiconductors, with a resistivity that decreases with increasing temperature (see figure 11).

Just like real superconductors, all holographic models exhibit zero conductivity when  $T < T_c$ . Interestingly, the temperature at which the resistivity becomes strictly zero is lower than the temperature  $T_c$  at which the non-abelian condensate becomes the true ground state. This is most clearly visible in figure 10. The small temperature range  $T_0 < T < T_c$  corresponds to a transition region where the resistivity very quickly drops from the normal-phase value to zero (the drop is more clearly visible in the real part of the conductivity, as the resistivity is suppressed by the large imaginary part).

When  $T > T_c$  only  $A_0 \neq 0$ , and hence only the abelian condensate  $\rho$  determines the behaviour of the system. The Yang-Mills truncation leads to a conductivity which is *independent* of the condensate (or chemical potential), due to the fact that the electromagnetic fluctuations fully decouple from the condensate in the abelian approximation. In this approximation, the system behaves as a semi-conductor, with a resistivity which decreases with increasing temperature (see figure 10). The DBI approximation, on the other hand, couples the fluctuations to the condensate, and leads to a condensate-dependent result for the conductivity [20],

$$\sigma^2 = aT^2 + \frac{\rho^2}{\lambda} \frac{b}{T^4}, \quad (4.12)$$

where  $a$  and  $b$  are numerical constants and  $\lambda$  is the 't Hooft coupling. The first, condensate-independent term originates from charge carriers that are thermally produced in charge neutral pairs, while the second term originates from the charge carriers introduced by the abelian condensate. The first term was visible in the Yang-Mills approximation and leads to semiconducting behaviour (an increase of temperature enhances thermal pair production), while the second term describes metallic behaviour.

The system thus behaves as a metal below the temperature  $T < T_*$ ,

$$T_* = \left( \frac{2\rho^2 b}{a\lambda} \right)^{1/6}, \quad (4.13)$$

which is governed by  $\alpha'$  corrections to the Yang-Mills action. As the system is cooled, the question is whether metallic behaviour will kick in before the superconducting phase or not. Obviously, this depends on whether  $T_c$  is smaller or larger than  $T_*$ . The requirement that  $T_* > T_c$ , i.e. that the system behaves as a metal above  $T_c$ , will put constraints on  $\lambda$ , and determine if it is compatible with the requirement that  $\lambda \ll 1$ . Of course, one should keep in mind that our analysis for  $T < T_c$  has been done in the (non-abelian) Yang-Mills approximation, while the analysis for  $T > T_c$  was done in the DBI approximation. Therefore, the first step one should take is to see how higher-derivative corrections could change the critical temperature. We leave this issue for future investigation.

## Acknowledgements

We would like to thank Imperial College for hospitality while parts of this paper were being written.

## A. Appendix: computing temperature dependence

While the coupled system of equations (2.9) is complicated and does not generically admit analytic solutions, it does have a useful scaling symmetry (both in the conformal and nonconformal cases), which simplifies our analysis. When considering a non-conformal systems we deal with three dimensionful parameters, the scale  $L$ , the temperature  $T$  and the chemical potential  $\mu$ . One might thus expect that the dimensionless condensate is a function of the two dimensionless combinations  $TL$  and  $\mu L$ . However, the equations (2.9) allow us to reduce this dependence to only one dimensionless combination  $\mu/T$ , with all  $TL$  dependence following from general arguments. This is a consequence of a scaling symmetry of (2.9), even when the metric (2.2) does not have conformal symmetry.

To see this, let us introduce a dimensionless radial coordinate  $\tilde{r} = r/r_T$ . In this coordinate the equations that determine the condensate read

$$\begin{aligned} \partial_{\tilde{r}} \left( h_1(\tilde{r}) \partial_{\tilde{r}} A_0^{(3)} \right) &= 4(A_3^{(1)})^2 A_0^{(3)} h_2(\tilde{r}) T^{-2}, \\ \partial_{\tilde{r}} \left( h_3(\tilde{r}) \partial_{\tilde{r}} A_3^{(1)} \right) &= 4(A_0^{(3)})^2 A_3^{(1)} h_4(\tilde{r}) T^{-2}, \end{aligned} \quad (A.1)$$

where the  $h_i(\tilde{r})$  are functions of  $\tilde{r}$  only. That is, all  $T$ -dependence sits in the explicit  $T^{-2}$  factor of the terms on the right-hand side, and there is no bare dependence on  $L$  anymore. Solutions to the equations now take the form

$$A_0^{(3)} = \mu + \rho r^\alpha + \dots = T \left( \tilde{\mu} + \tilde{\rho} \tilde{r}^\alpha + \dots \right) =: T \tilde{A}_0^{(3)}, \quad (A.2)$$

and similar for  $A_3^{(1)}$  (see e.g. (A.4) for the D4/D8 case). Here  $\alpha$  is a model-dependent constant and we have defined

$$\tilde{\mu} := \frac{\mu}{T} \quad \text{and} \quad \tilde{\rho} := \frac{\rho(r_T)^\alpha}{T}. \quad (\text{A.3})$$

From the fact that the equations (A.1) are independent of  $T$  and  $L$  when expressed in terms of the  $\tilde{A}_0^{(3)}$  and  $\tilde{A}_3^{(1)}$  variables, we can then conclude that the dimensionless quantity  $\tilde{\rho}$  only depends on  $\tilde{\mu}$ , not on the dimensionless combination  $TL$ . For the D4/D8 system, for instance, the expansion reads

$$\text{D4/D8 :} \quad A_0^{(3)} = T \left[ \frac{\mu}{T} - \frac{\rho}{T^{5/2}(TL)^{3/2}} \tilde{r}^{3/2} + \dots \right] =: T \left[ \tilde{\mu} - \tilde{\rho} \tilde{r}^{3/2} + \dots \right]. \quad (\text{A.4})$$

So we see that even when the theory is not conformally invariant<sup>8</sup>, the scaling symmetry of the equations allows us to determine the dependence of the dimensionless condensate on  $TL$ . We also note that if one were to include higher derivative terms into the equations of motion (which for example follow from the DBI action), then the above symmetry would not necessarily continue to be present. In practice, we have used the scaling symmetry to verify numerical stability of the condensate solutions: plots of  $\tilde{\mu}$  against  $\tilde{\rho}$  should be independent of  $TL$ .

The scaling argument also allows us to determine e.g. the temperature dependence of the action by changing  $\mu$  instead of  $r_T$ . The idea here is to compute the action in  $\tilde{r}$  coordinates at a fixed value  $r_T = 1$ . This will yield  $S(\mu, T) = r_T^\beta \tilde{S}(\mu/T, r_T = 1)$  for some  $\beta$ , with the overall power of  $r_T$  simply arising from the coordinate transformation  $r = r_T \tilde{r}$ . We will see this at work in section 3.1.

---

<sup>8</sup>In the conformal D3/D7 case, this story simplifies and the dimensionless condensate  $\rho/T$  is independent of  $TL$ , but the argument presented here shows that the story is somewhat more complicated in the non-conformal cases, where the naive dimensionless combination  $\rho/T^{(\alpha+1)}$  still depends on  $TL$ , albeit only in the simple way dictated by (A.3).

## References

- [1] S. A. Hartnoll, C. P. Herzog, and G. T. Horowitz, “Building a holographic superconductor”, *Phys. Rev. Lett.* **101** (2008) 031601, [arXiv:0803.3295](#).
- [2] S. A. Hartnoll, “Lectures on holographic methods for condensed matter physics”, [arXiv:0903.3246](#).
- [3] C. P. Herzog, “Lectures on holographic superfluidity and superconductivity”, [arXiv:0904.1975](#).
- [4] S. S. Gubser and S. S. Pufu, “The gravity dual of a p-wave superconductor”, *JHEP* **11** (2008) 033, [arXiv:0805.2960](#).
- [5] S. A. Hartnoll, C. P. Herzog, and G. T. Horowitz, “Holographic superconductors”, *JHEP* **12** (2008) 015, [arXiv:0810.1563](#).
- [6] O. Aharony, K. Peeters, J. Sonnenschein, and M. Zamaklar, “Rho meson condensation at finite isospin chemical potential in a holographic model for QCD”, *JHEP* **082** (2007) 1007, [arXiv:0709.3948](#).
- [7] S. S. Gubser, “Colorful horizons with charge in anti-de Sitter space”, *Phys. Rev. Lett.* **101** (2008) 191601, [arXiv:0803.3483](#).
- [8] M. Kulaxizi and A. Parnachev, “Holographic responses of fermion matter”, *Nucl. Phys.* **B815** (2009) 125–141, [arXiv:0811.2262](#).
- [9] A. Karch, D. T. Son, and A. O. Starinets, “Zero sound from holography”, [arXiv:0806.3796](#).
- [10] J. Erdmenger and I. Kirsch, “Mesons in gauge/gravity dual with large number of fundamental fields”, *JHEP* **12** (2004) 025, [hep-th/0408113](#).
- [11] T. Sakai and S. Sugimoto, “Low energy hadron physics in holographic QCD”, *Prog. Theor. Phys.* **113** (2005) 843–882, [hep-th/0412141](#).
- [12] S. S. Gubser and F. D. Rocha, “The gravity dual to a quantum critical point with spontaneous symmetry breaking”, *Phys. Rev. Lett.* **102** (2009) 061601, [arXiv:0807.1737](#).
- [13] S. S. Gubser and A. Nellore, “Low-temperature behavior of the Abelian Higgs model in anti-de Sitter space”, *JHEP* **04** (2009) 008, [arXiv:0810.4554](#).
- [14] O. Aharony, J. Sonnenschein, and S. Yankielowicz, “A holographic model of deconfinement and chiral symmetry restoration”, *Ann. Phys.* **322** (2007) 1420–1443, [hep-th/0604161](#).
- [15] M. Ammon, J. Erdmenger, M. Kaminski, and P. Kerner, “Flavor superconductivity from gauge/gravity duality”, [arXiv:0903.1864](#).

- [16] A. Tari, “The specific heat of matter at low temperatures”, Imperial College Press, 2003.
- [17] N. E. Phillips, “Low-temperature heat capacities of gallium, cadmium, and copper”, *Phys. Rev.* **A385** (1964) 134.
- [18] H. R. Ott, H. Rudigier, T. M. Rice, K. Ueda, Z. Fisk, and J. L. Smith, “ $p$ -Wave superconductivity in  $\text{UBe}_{13}$ ”, *Phys. Rev. Lett.* **52** (1984) 1915.
- [19] P. S. Riseborough, G. M. Schmiedeshoff, and J. L. Smith, “Heavy-fermion superconductivity”, in “Superconductivity volume II: novel superconductors”, K. H. Bennemann and J. B. Ketterson, eds., ch. 19, p. 1031. Springer, 2008.
- [20] A. Karch and A. O’Bannon, “Metallic AdS/CFT”, *JHEP* **09** (2007) 024, [arXiv:0705.3870](#).
- [21] G. T. Horowitz and M. M. Roberts, “Holographic superconductors with various condensates”, *Phys. Rev.* **D78** (2008) 126008, [arXiv:0810.1077](#).
- [22] P. Basu, J. He, A. Mukherjee, and H.-H. Shieh, “Superconductivity from D3/D7: holographic pion superfluid”, [arXiv:0810.3970](#).
- [23] F. Marsiglio and J. P. Carbotte, “Electron-phonon superconductivity”, in “Superconductivity volume I: conventional and unconventional superconductors”, K. H. Bennemann and J. B. Ketterson, eds., ch. 3, p. 73. Springer, 2008.
- [24] N. Iqbal and H. Liu, “Universality of the hydrodynamic limit in AdS/CFT and the membrane paradigm”, *Phys. Rev.* **D79** (2009) 025023, [arXiv:0809.3808](#).
- [25] S. Caron-Huot, P. Kovtun, G. D. Moore, A. Starinets, and L. G. Yaffe, “Photon and dilepton production in supersymmetric Yang-Mills plasma”, *JHEP* **12** (2006) 015, [hep-th/0607237](#).
- [26] H. R. Ott, H. Rudigier, Z. Fisk, and J. L. Smith, “ $\text{UBe}_{13}$ : An unconventional actinide superconductor”, *Phys. Rev. Lett.* **50** (1983) 1595.